Direction-of-Arrival Estimation in the Low-SNR Regime via a Denoising Autoencoder

Mathini Sellathurai, Georgios K. Papageorgiou

Heriot-Watt University, School of Engineering and Physical Sciences, Edinburgh, UK

UDRC Themed Meeting on Signal Processing for the Electromagnetic Environment

UDRC 3

The research was funded by UK EPSRC grant EP/P009670/1 and MBDA

Outline

Case 1: Signal Model - Uniform Linear Arrays (ULA)

We consider an N-element half-wavelength spaced ULA for the direction-of-arrival (DoA) estimation of K far-field, distinct and uncorrelated sources.

Received Signal

$$\mathbf{x}(t) = \sum_{k=1}^{K} \mathbf{a}(\theta_k) s_k(t) + \mathbf{e}(t) = \mathbf{A}(\mathbf{f})\mathbf{s}(t) + \mathbf{e}(t), \ t = 1, \ldots, T,$$

where $\mathbf{A}(\mathbf{f}) = [\mathbf{a}(f_1), \mathbf{a}(f_2), \ldots, \mathbf{a}(f_K)]$ is the $N \times K$ array manifold matrix with columns $\mathbf{a}(f_k) = [1, f_k, f_k^2, \ldots, f_k^{N-1}]^T$, $f_k = e^{\mathrm{j}\pi \sin\theta_k}$ and θ_k are the DoAs for $k = 1, \ldots, K$. The transmitted signal is $\mathbf{s}(t) = [s_1(t), \ldots, s_K(t)]^T$ and $\mathbf{e}(t) \sim \mathcal{CN}(\mathbf{0}, \sigma_e^2 \mathbf{I}_N)$ is the noise vector.

Additional Assumptions:

- The additive noise values are i.i.d. zero-mean white circularly-symmetric Gaussian and uncorrelated from the sources.
- There is no temporal correlation between the snapshots.

Case 1: Signal Model - Uniform Linear Arrays (ULA)

We consider an N-element half-wavelength spaced ULA for the direction-of-arrival (DoA) estimation of K far-field, distinct and uncorrelated sources.

Received Signal

$$\mathbf{x}(t) = \sum_{k=1}^{K} \mathbf{a}(\theta_k) s_k(t) + \mathbf{e}(t) = \mathbf{A}(\mathbf{f})\mathbf{s}(t) + \mathbf{e}(t), \ t = 1, \ldots, T,$$

where $\mathbf{A}(\mathbf{f}) = [\mathbf{a}(f_1), \mathbf{a}(f_2), \ldots, \mathbf{a}(f_K)]$ is the $N \times K$ array manifold matrix with columns $\mathbf{a}(f_k) = [1, f_k, f_k^2, \ldots, f_k^{N-1}]^T$, $f_k = e^{\mathrm{j}\pi \sin\theta_k}$ and θ_k are the DoAs for $k = 1, \ldots, K$. The transmitted signal is $\mathbf{s}(t) = [s_1(t), \ldots, s_K(t)]^T$ and $\mathbf{e}(t) \sim \mathcal{CN}(\mathbf{0}, \sigma_e^2 \mathbf{I}_N)$ is the noise vector.

Additional Assumptions:

- The additive noise values are i.i.d. zero-mean white circularly-symmetric Gaussian and uncorrelated from the sources.
- There is no temporal correlation between the snapshots.

Under these assumptions the source covariance matrix is $\mathbf{R}_s = \mathbb{E}[\mathbf{s}(t)\mathbf{s}^H(t)] = \text{diag}(p_1, \ldots, p_K)$ and the received signal's covariance matrix is:

Covariance Matrix of the Received Signal

$$\mathbf{R}_x = \mathbb{E}[\mathbf{x}(t)\mathbf{x}^H(t)] = \mathbf{A}(\mathbf{f})\mathbf{R}_s\mathbf{A}^H(\mathbf{f}) + \sigma_e^2\mathbf{I}_N.$$

Facts and Challenges:

- Conventional subspace-based approaches, such as Multiple Signal Classification (MUSIC), rely on the eigendecomposition $\mathbf{R}_x = \mathbf{U}\mathbf{\Sigma}\mathbf{U}^H$ for the signal and noise subspace separation.
- In practice, $\mathbf{R}_x$ is unknown and estimation is performed via its sample estimate $\widetilde{\mathbf{R}}_x = \frac{1}{T}\sum_{t=1}^{T}\mathbf{x}(t)\mathbf{x}^H(t)$, for a number of snapshots T.
- Up to $K \leq N-1$ distinct DoAs can be estimated with guarantees in the noiseless case. In the presence of noise, no conditions guarantee the DoA estimation, which depends on both T and the signal-to-noise-ration (SNR).

Under these assumptions the source covariance matrix is $\mathbf{R}_s = \mathbb{E}[\mathbf{s}(t)\mathbf{s}^H(t)] = \text{diag}(p_1, \ldots, p_K)$ and the received signal's covariance matrix is:

Covariance Matrix of the Received Signal

$$\mathbf{R}_x = \mathbb{E}[\mathbf{x}(t)\mathbf{x}^H(t)] = \mathbf{A}(\mathbf{f})\mathbf{R}_s\mathbf{A}^H(\mathbf{f}) + \sigma_e^2\mathbf{I}_N.$$

Facts and Challenges:

- Conventional subspace-based approaches, such as Multiple Signal Classification (MUSIC), rely on the eigendecomposition $\mathbf{R}_x = \mathbf{U}\mathbf{\Sigma}\mathbf{U}^H$ for the signal and noise subspace separation.
- In practice, $\mathbf{R}_x$ is unknown and estimation is performed via its sample estimate $\widetilde{\mathbf{R}}_x = \frac{1}{T}\sum_{t=1}^{T}\mathbf{x}(t)\mathbf{x}^H(t)$, for a number of snapshots T.
- Up to $K \leq N-1$ distinct DoAs can be estimated with guarantees in the noiseless case. In the presence of noise, no conditions guarantee the DoA estimation, which depends on both T and the signal-to-noise-ration (SNR).

Case 2: Signal Model for Sparse Linear Arrays

Sparse Linear Arrays (SLAs) are a class of nonuniform linear arrays (NLAs). Typically, SLAs comprise a small number of sensors from a larger aperture Uniform Linear Array (ULA). The subset of sensors selected depends on the type of the SLA:

- Minimum Redundancy Arrays (MRAs) - (M. Ishiguro, 1980)
  - Maximizes the number of consecutive virtual sensors in the difference coarray.
  - No closed-form expressions exist for a) the sensor locations and b) the number of achievable degrees-of-freedom (DoF).
- Nested Arrays - (P. Pal and P. Vaidyanathan, 2010)
  - Closed-form expressions exist and can provide $\mathcal{O}(N^2)$ DoF with N physical sensors.
  - The number of DoF is smaller than that of the MRA.
  - Higher level of nesting can increase the DoFs but the difference coarray is not necessarily a hole-free ULA.

Case 2: Signal Model for Sparse Linear Arrays

Sparse Linear Arrays (SLAs) are a class of nonuniform linear arrays (NLAs). Typically, SLAs comprise a small number of sensors from a larger aperture Uniform Linear Array (ULA). The subset of sensors selected depends on the type of the SLA:

- Minimum Redundancy Arrays (MRAs) - (M. Ishiguro, 1980)
  - Maximizes the number of consecutive virtual sensors in the difference coarray.
  - No closed-form expressions exist for a) the sensor locations and b) the number of achievable degrees-of-freedom (DoF).
- Nested Arrays - (P. Pal and P. Vaidyanathan, 2010)
  - Closed-form expressions exist and can provide $\mathcal{O}(N^2)$ DoF with N physical sensors.
  - The number of DoF is smaller than that of the MRA.
  - Higher level of nesting can increase the DoFs but the difference coarray is not necessarily a hole-free ULA.

Case 2: Signal Model for Sparse Linear Arrays (cont.)

Types of arrays (continued):

- Co-prime Arrays - (P. Pal and P. P. Vaidyanathan, 2011)
  - The mutual coupling effects between elements is reduced compared to the nested arrays.
  - The number of DoF is smaller than that of the nested arrays (for the same number of sensors).
- Augmented Nested Arrays (ANA) - (J. Liu et al., 2017)
  - Higher number of DoF.
  - more effective against mutual coupling but hole-free under certain complicated conditions.
- Maximum Inter-element Spacing Constraint (MISC) Arrays - (Z. Zheng et al., 2019)
  - Reduced mutual coupling.
  - Closed-form expressions for the locations and achievable DoFs.
  - It has been proved that the difference coarray is always hole-free.
  - Increased number of DoFs on the virtual array.

Case 2: Signal Model for Sparse Linear Arrays (cont.)

Types of arrays (continued):

- Co-prime Arrays - (P. Pal and P. P. Vaidyanathan, 2011)
  - The mutual coupling effects between elements is reduced compared to the nested arrays.
  - The number of DoF is smaller than that of the nested arrays (for the same number of sensors).
- Augmented Nested Arrays (ANA) - (J. Liu et al., 2017)
  - Higher number of DoF.
  - more effective against mutual coupling but hole-free under certain complicated conditions.
- Maximum Inter-element Spacing Constraint (MISC) Arrays - (Z. Zheng et al., 2019)
  - Reduced mutual coupling.
  - Closed-form expressions for the locations and achievable DoFs.
  - It has been proved that the difference coarray is always hole-free.
  - Increased number of DoFs on the virtual array.

Case 2: Signal Model for Sparse Linear Arrays (cont.)

Types of arrays (continued):

- Co-prime Arrays - (P. Pal and P. P. Vaidyanathan, 2011)
  - The mutual coupling effects between elements is reduced compared to the nested arrays.
  - The number of DoF is smaller than that of the nested arrays (for the same number of sensors).
- Augmented Nested Arrays (ANA) - (J. Liu et al., 2017)
  - Higher number of DoF.
  - more effective against mutual coupling but hole-free under certain complicated conditions.
- Maximum Inter-element Spacing Constraint (MISC) Arrays - (Z. Zheng et al., 2019)
  - Reduced mutual coupling.
  - Closed-form expressions for the locations and achievable DoFs.
  - It has been proved that the difference coarray is always hole-free.
  - Increased number of DoFs on the virtual array.

Maximum Inter-element Spacing Constraint Array

MISC Array

For an arbitrary number of sensors N with $N \geq 5$ they are constructed based on the maximum inter-element spacing $P = 2\lfloor \frac{N}{4} \rfloor + 2$, which determines the following inter-element spacing set:

$$\mathcal{A}_{\text{MISC}}(N) = \{1, P-3, \underbrace{P, \ldots, P}_{N-P}, \underbrace{2, \ldots, 2}_{\frac{P-4}{2}}, 3, \underbrace{2, \ldots, 2}_{\frac{P-4}{2}}\}.$$

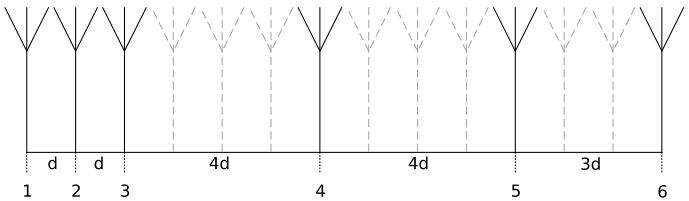

Figure: An example of the MISC array with $N = 6$ (thus, $P = 4$) elements as a sparse version of a larger ULA (57% fewer elements). Inter-element spacing defined by the set: $\mathcal{A}_{\text{MISC}}(6) = \{1, 1, 4, 4, 3\}$ and locations by the set $\mathcal{S}_{\text{MISC}}(6) = \{0, 1, 2, 6, 10, 13\}d$. The dashed elements correspond to missing sensors. It can also be viewed as an efficient way to sample the array domain.

Maximum Inter-element Spacing Constraint Array

MISC Array

For an arbitrary number of sensors N with $N \geq 5$ they are constructed based on the maximum inter-element spacing $P = 2\lfloor \frac{N}{4} \rfloor + 2$, which determines the following inter-element spacing set:

$$\mathcal{A}_{\text{MISC}}(N) = \{1, P-3, \underbrace{P, \ldots, P}_{N-P}, \underbrace{2, \ldots, 2}_{\frac{P-4}{2}}, 3, \underbrace{2, \ldots, 2}_{\frac{P-4}{2}}\}.$$

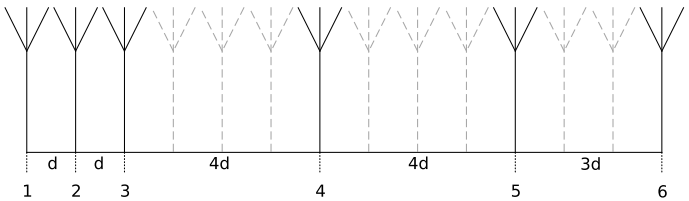

Figure: An example of the MISC array with $N = 6$ (thus, $P = 4$) elements as a sparse version of a larger ULA (57% fewer elements). Inter-element spacing defined by the set: $\mathcal{A}_{\text{MISC}}(6) = \{1, 1, 4, 4, 3\}$ and locations by the set $\mathcal{S}_{\text{MISC}}(6) = \{0, 1, 2, 6, 10, 13\}d$. The dashed elements correspond to missing sensors. It can also be viewed as an efficient way to sample the array domain.

Direction-of-Arrival (DoA) Estimation with SLAs

DoA estimation of K targets/sources with N physical sensors:

- Overdetermined case ($K < N$): Conventional covariance-based techniques, e.g., Multiple SIgnal Classification (MUSIC).
- Underdetermined case ($K \geq N$): First perform Spatial Smoothing (SS) and then use a covariance-based technique.

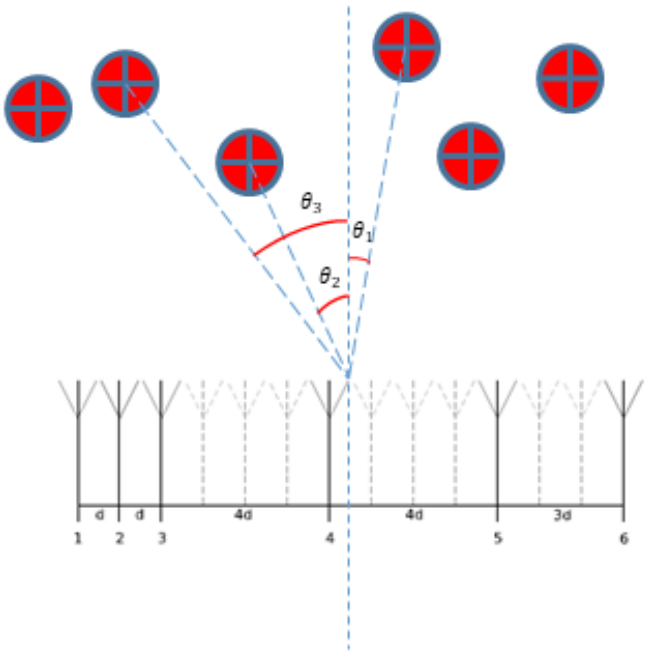

Despite having $N = 6$ physical sensors the number of the (uniform) DoFs for the virtual array is $N_{\mathrm{v}} = 27$, enabling the DoA estimation of a larger number of targets/sources.

Direction-of-Arrival (DoA) Estimation with SLAs

DoA estimation of K targets/sources with N physical sensors:

- Overdetermined case ($K < N$): Conventional covariance-based techniques, e.g., Multiple SIgnal Classification (MUSIC).
- Underdetermined case ($K \geq N$): First perform Spatial Smoothing (SS) and then use a covariance-based technique.

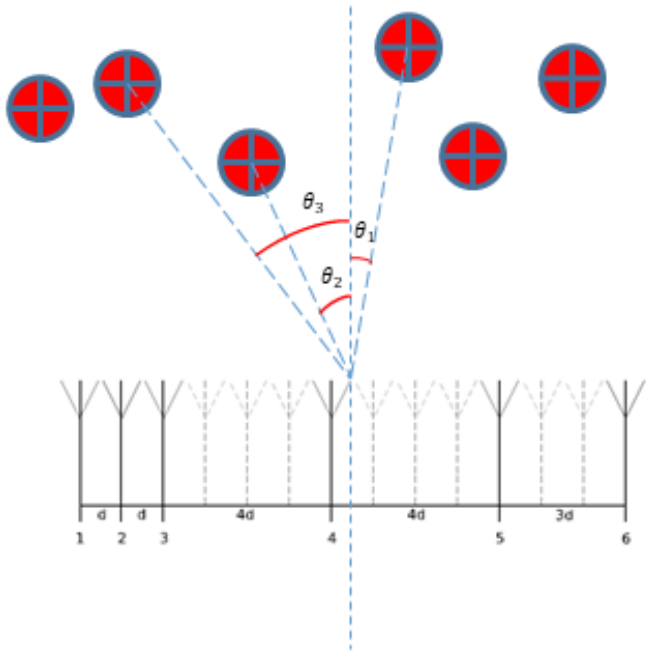

Despite having $N = 6$ physical sensors the number of the (uniform) DoFs for the virtual array is $N_{\mathrm{v}} = 27$, enabling the DoA estimation of a larger number of targets/sources.

Sample Covariance Matrix

$$\widetilde{\mathbf{R}}_x = \mathbf{R}_x + \Delta\mathbf{R},$$

where $\Delta\mathbf{R} = \mathbf{A}(\mathbf{f})\Delta\mathbf{R}_s\mathbf{A}^H(\mathbf{f}) + \mathbf{A}(\mathbf{f})\widetilde{\mathbf{R}}_{se} + \widetilde{\mathbf{R}}_{se}^H\mathbf{A}^H(\mathbf{f}) + \Delta\mathbf{R}_e$, $\widetilde{\mathbf{R}}_{se}$ is the signal-noise sample cross-covariance matrix, $\Delta\mathbf{R}_s = \widetilde{\mathbf{R}}_s - \mathbf{R}_s$, $\Delta\mathbf{R}_e = \widetilde{\mathbf{R}}_e - \sigma_e^2\mathbf{I}_N$ and $\widetilde{\mathbf{R}}_s, \widetilde{\mathbf{R}}_e$ are the signal and noise sample covariance matrices, respectively.

- For $T \to \infty$, $\widetilde{\mathbf{R}}_s \to \mathbf{R}_s, \widetilde{\mathbf{R}}_{s\eta} \to \mathbf{O}$ and $\widetilde{\mathbf{R}}_\eta \to \sigma_\eta^2\mathbf{I}_N$ leading to $\Delta\mathbf{R} \to \mathbf{O}$.
- The values of $\Delta\mathbf{R}$ depend on both T and the SNR. In the low-SNR regime even a large (but finite) number of snapshots cannot reduce these error values significantly.

- $\mathrm{vt}(\cdot) = [\mathrm{vtr}(\cdot)^T, \mathrm{vti}(\cdot)^T]^T$ maps the Hermitian matrix to a composite real-valued vector and the reverse operator, $\mathrm{uvt}(\cdot)$, maps the $N^2 \times 1$ real-valued vector back into the complex-valued Hermitian matrix.
- For example, the Hermitian matrix

$$\mathbf{R} = \begin{bmatrix} a_1 & a_2 + \mathrm{j}a_3 & a_4 + \mathrm{j}a_5 \\ a_2 - \mathrm{j}a_3 & b_1 & b_2 + \mathrm{j}b_3 \\ a_4 - \mathrm{j}a_5 & b_2 - \mathrm{j}b_3 & c_1 \end{bmatrix} \text{ of } \mathbb{C}^{3\times 3} \text{ with}$$

$\{a_1, \ldots, a_5, b_1, b_2, b_3, c1\} \in \mathbb{R}$ has:

- $\mathrm{vtr}(\mathbf{R}) = [a_1, a_2, b_1, a_4, b_2, c_1]^T$ and $\mathrm{vti}(\mathbf{R}) = [a_3, a_5, b_3]^T$. Hence,

$$\mathrm{vt}(\mathbf{R}) = [a_1, a_2, b_1, a_4, b_2, c_1, a_3, a_5, b_3]^T \in \mathbb{R}^{9\times 1}.$$

- Applying the $\mathrm{vt}(\cdot)$ operator to the sample covariance matrix leads to $\widetilde{\mathbf{r}} = \mathbf{r} + \Delta\mathbf{r}$, where $\widetilde{\mathbf{r}} = \mathrm{vt}(\widetilde{\mathbf{R}}_x)$, $\mathbf{r} = \mathrm{vt}(\mathbf{R}_x)$ and $\Delta\mathbf{r} = \mathrm{vt}(\Delta\mathbf{R})$.

Objective: Learn $\mathbf{r}$ from $\widetilde{\mathbf{r}} = \mathbf{r} + \Delta\mathbf{r}$

- For sufficient number of snapshots T the sample covariance estimate is statistically optimal in the high-SNR regime.
- However, in many practical applications, the signal is buried in noise (low-SNR regime) and the data in $\widetilde{\mathbf{r}}$ lie far away from the true unknown manifold (data points in $\mathbf{r}$). As a result, the majority of the estimators fail to accurately estimate the DoAs in such cases.

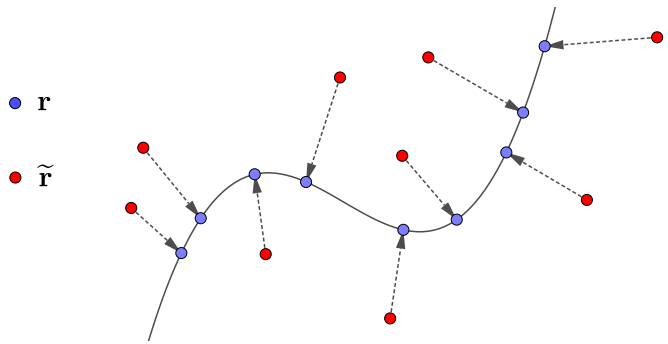

Proposed solution: train a Denoising Autoencoder (DAE) to "learn" the unknown manifold.

Learning Hermitian Matrices

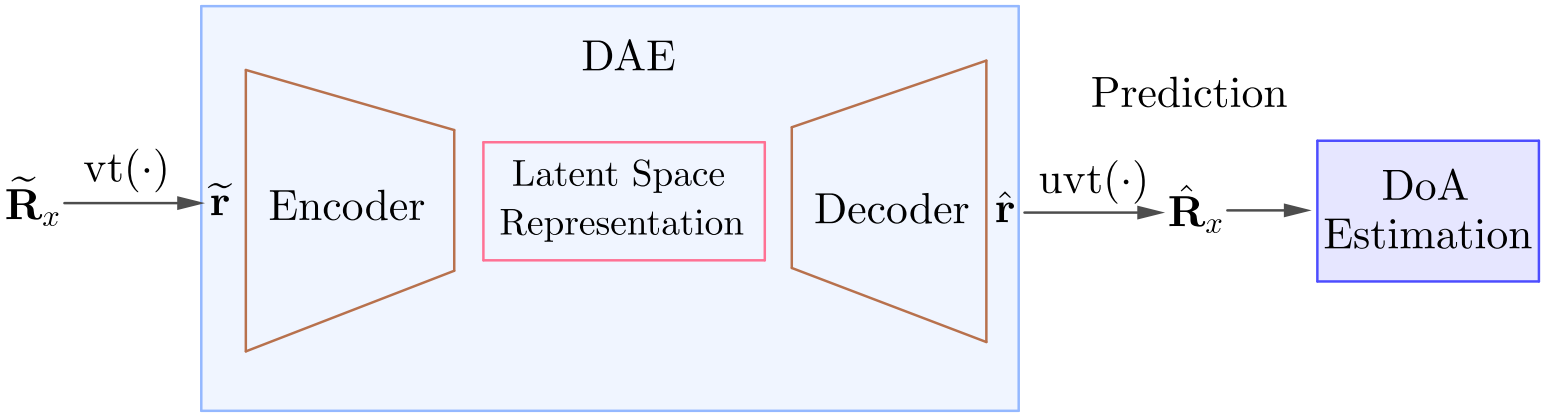

Figure: The proposed DL-based prediction scheme. The Denoising Autoencoder (DAE) learns to predict $\hat{\mathbf{r}}$, which is then mapped to a Hermitian matrix $\hat{\mathbf{R}}_x$. The latter matrix can then be used by one/any of the covariance-based methods for DoA estimation available in the literarure.

Denoising Autoencoder Loss

$$\{\vartheta^*, \vartheta'^*\} = \arg\min_{\vartheta,\vartheta'} \left\{ \frac{1}{D} \sum_{d=1}^{D} \mathcal{L}\left(\mathbf{r}^{(d)}, g_{\vartheta'}\left(f_{\vartheta}\left(\widetilde{\mathbf{r}}^{(d)} \right) \right) \right) + \frac{\lambda}{2D} \left(\sum_{m=1}^{M} \|\mathbf{W}_m\|_F^2 + \sum_{\ell=1}^{L} \|\mathbf{W}'_\ell\|_F^2 \right) \right\},$$

where $\mathcal{L}(\cdot)$ is the MSE loss and λ is a regularization parameter.

Weights-biases: $\vartheta = \{\vartheta_m\}_{m=1}^{M}$ with $\vartheta_m = \{\mathbf{W}_m, \mathbf{b}_m\}$, $\vartheta' = \{\vartheta'_\ell\}_{\ell=1}^{L}$ with $\vartheta'_\ell = \{\mathbf{W'}_\ell, \mathbf{b'}_\ell\}$.

Functions: $f_\vartheta = f_{\vartheta_M} \circ f_{\vartheta_{M-1}} \cdots f_{\vartheta_1}$ with $f_{\vartheta_m}(\mathbf{x}) = \phi_{f_m}(\mathbf{b}_m + \mathbf{W}_m\mathbf{x})$ is the encoder with activation function ϕ_{f_m} at the m-th layer and $g_{\vartheta'} = g_{\vartheta'_L} \circ g_{\vartheta'_{L-1}} \cdots g_{\vartheta'_1}$ with $g_{\vartheta'_\ell}(\mathbf{x}) = \phi_{g_\ell}(\mathbf{b}'_\ell + \mathbf{W}'_\ell\mathbf{x})$ is the decoder with activation function ϕ_{g_ℓ} at the ℓ-th layer.

DAE Layout

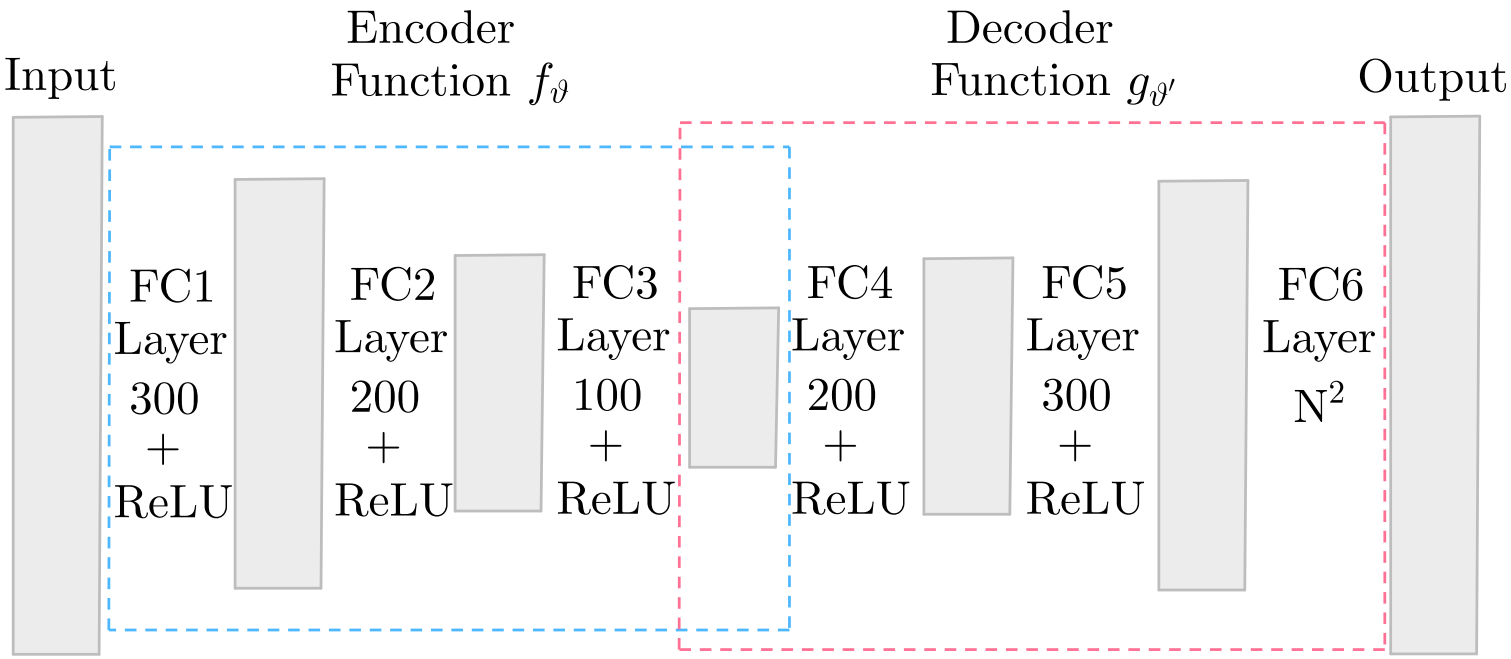

Figure: The proposed DAE architecture follows the standard bottleneck structure. The encoded dimension (of the latent space) is 100, whereas the input and output dimensions are N^2. In total, the DAE comprises six fully connected (FC) layers.

Fast DoA Prediction-estimation Scheme

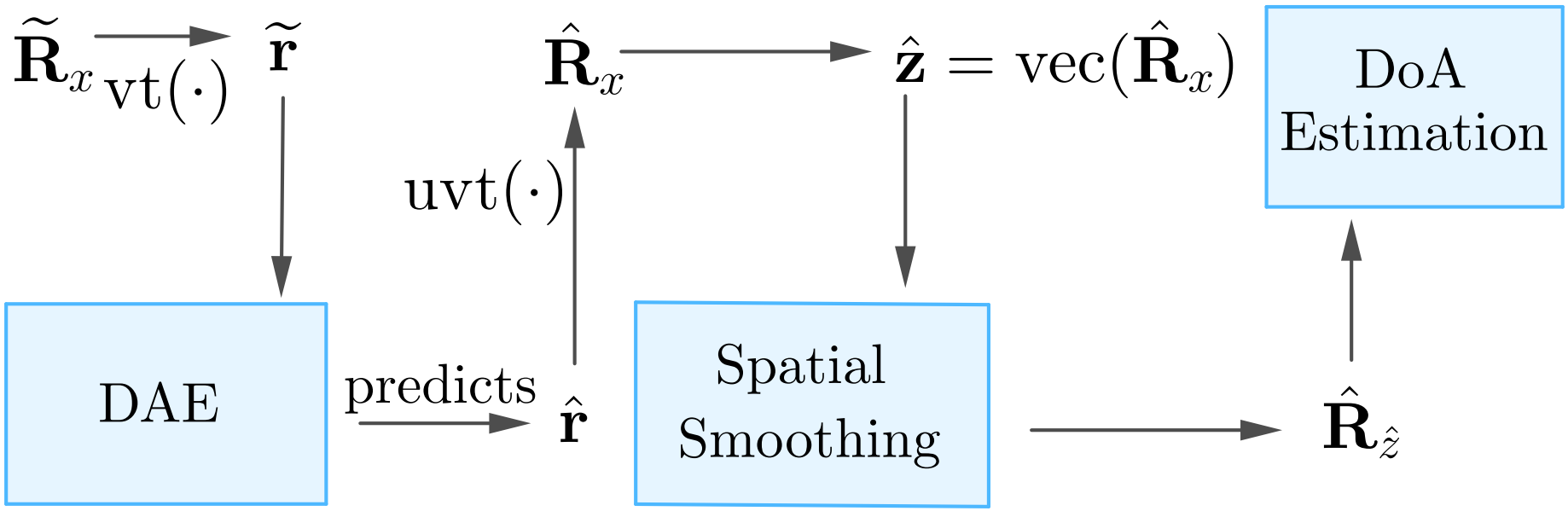

Figure: The proposed fast covariance matrix prediction scheme for DoA estimation. The noisy covariance matrix $\widetilde{\mathbf{R}}_x$ is passed to the DAE, which predicts $\hat{\mathbf{R}}_x$. For the underdetremined case using MISC, spatial smoothing is applied to the vectorized form. The DoA estimation is performed on $\hat{\mathbf{R}}_{\hat{z}}$ using a covariance-based technique, such as MUltiple SIgnal Classification (MUSIC).

Simulation Setup and Numerical Evaluation for Overdetermined Case $K < N - 1$ with ULA

Simulation Setup:

- ULA with $N = 20$ elements.
- $K = 2$ sources with $p_1 = p_2 = 1$ and the two DoAs in $[-80°, -5°]$ and $[5°, 80°]$, respectively.
- SNR in [-20,-5] dB, where SNR $= 10 \log_{10} \left(\min\{p_1, p_2\} / \sigma_e^2 \right)$.

DAE Training:

- Training with $D = 2$M data using $T_{\min} = 1000$ snapshots.
- Testing with $D_t = 100$K data using $T \geq T_{\min}$.
- SNR random.

Evaluation Metric:

Root-mean-squared-error (RMSE):

$$\text{RMSE} = \sqrt{\frac{1}{D_t K} \sum_{k=1}^{K} \sum_{d=1}^{D_t} (\theta_k^{(d)} - \hat{\theta}_k^{(d)})^2}.$$

Case $K < N - 1$ with ULA: RMSE vs SNR

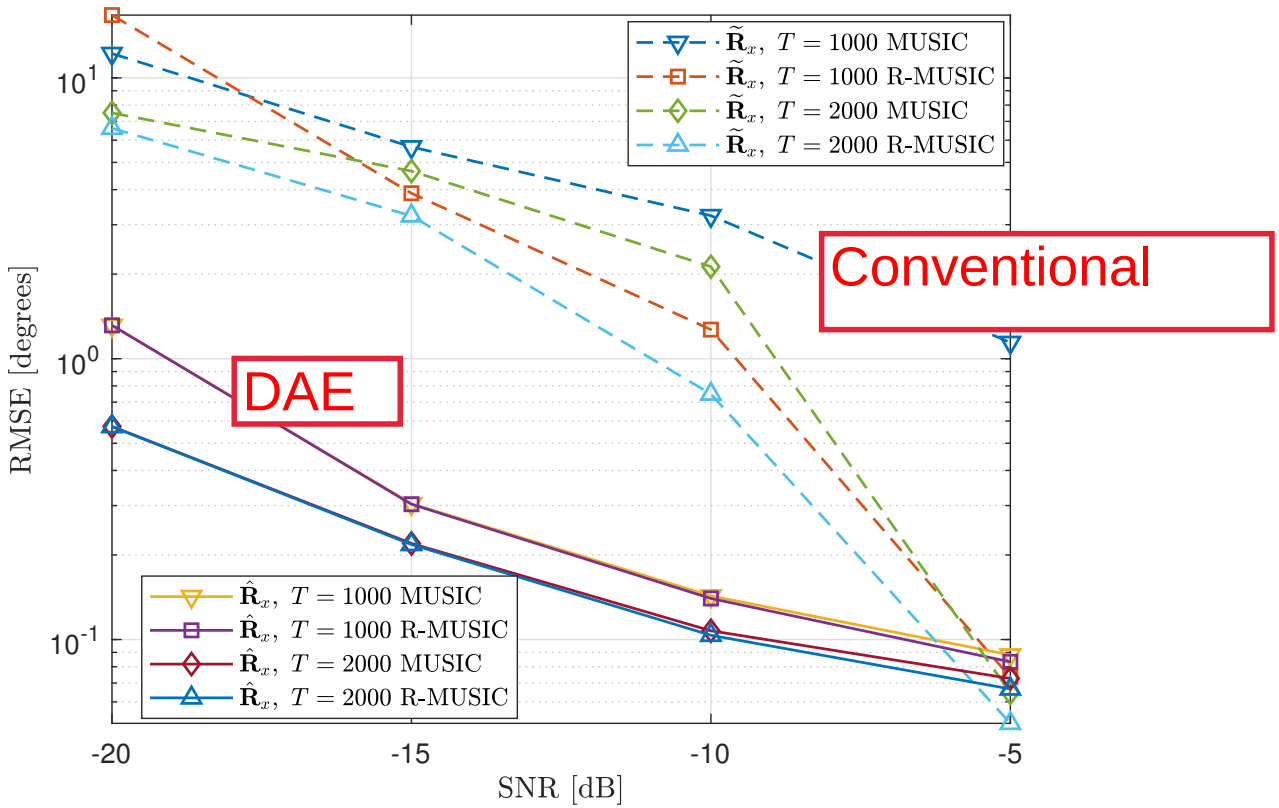

Figure: The RMSE (logarithmic scale) vs the SNR in the DoA estimation of two sources. The dashed lines correspond to the DoA estimation with the sample estimate, while the solid ones with the matrix predicted by the proposed DAE. The relative improvement is up to 95% (low-SNR).

Case $K < N - 1$ with ULA: RMSE vs T

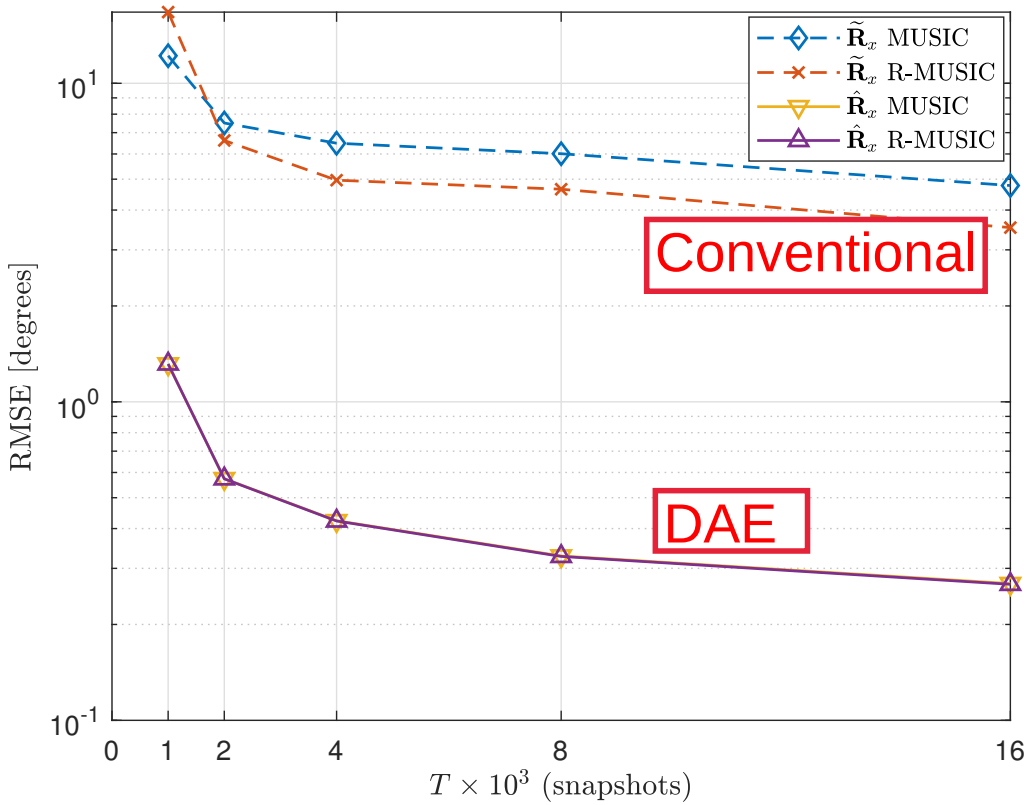

Figure: The RMSE (logarithmic scale) vs the number of snapshots T for the estimation of two DoAs at -20 dB. Notice that the increase in the number of snapshots has a greater impact on the DoA estimation with the predicted matrix $\hat{\mathbf{R}}_x$ than with the conventional sample estimate $\widetilde{\mathbf{R}}_x$.

Underdetermined case $K > N - 1$: Parameters

Table: Layers of the DAE

Layer	Size	Activation
Fully Connected	1000	RELU
Fully Connected	800	RELU
Fully Connected	300	RELU
Fully Connected	100	RELU
Fully Connected	300	RELU
Fully Connected	800	RELU
Fully Connected	1000	RELU
Fully Connected	N^2	LINEAR

Table: Parameters used for the numerical evaluation

Parameter	Value
Sensors N	6
Sources K	6
Train data D	500K
Test data D_t	75K
λ	10^{-4}

Case $K > N - 1$: Probability of Detection for On-grid Angles

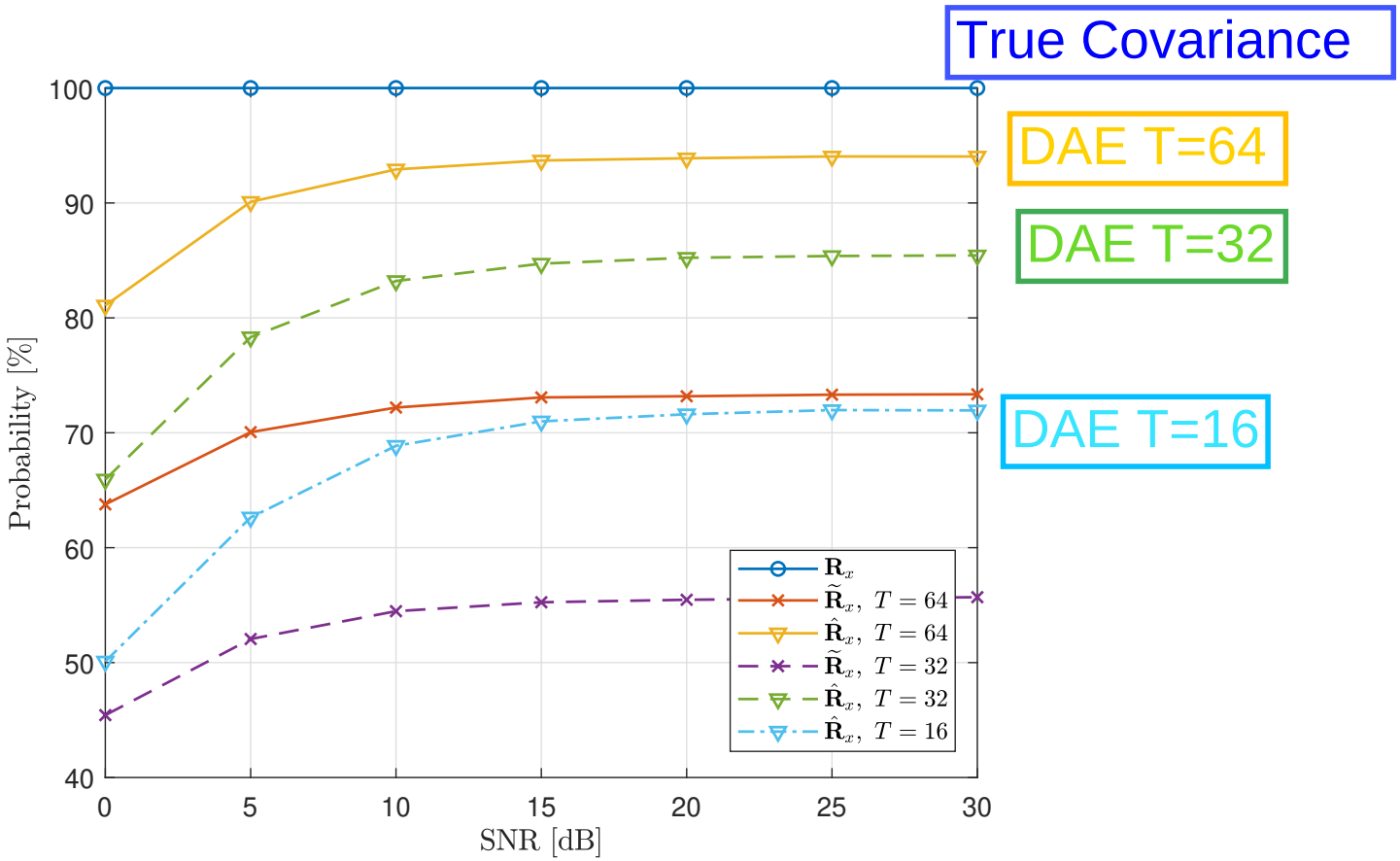

Figure: The probabilities of detection of $K = 6$ targets using $N = 6$ physical sensors with MUSIC vs the SNR for angles on a discrete grid. For $T = 16$ the angles can only be resolved with the use of the proposed DAE.

Case $K > N - 1$: RMSE for Off-grid Angles

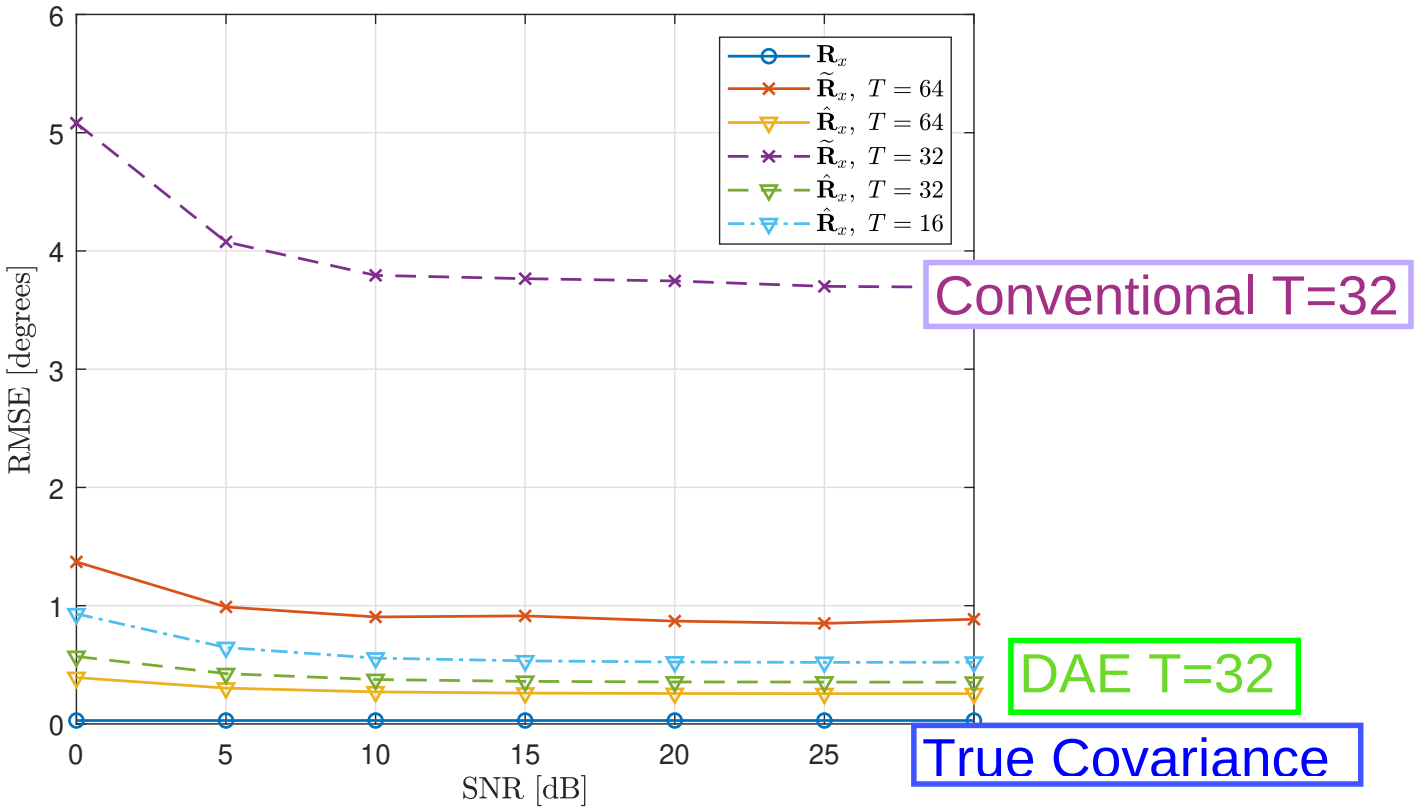

Figure: The RMSE in the estimation of $K = 6$ targets using $N = 6$ physical sensors with MUSIC vs the SNR for randomly selected angles. For $T = 16$ the angles are not resolved by the conventional approach.

Conclusions

- We presented a novel deep learning approach for DoA estimation for 1) low SNR, 2) small number of snapshots T, and we focused on the overdetermined ($K < N - 1$) and underdetermined case ($K \geq N$) using the ULA and MISC arrays, respectively.
- The problem is formulated as a manifold learning task and a (deep) denoising autoencoder architecture is trained for the prediction of the true (unknown) manifold. The DoA estimation follows with the use of a conventional covariance-based technique.
- The adopted approach demonstrates significant performance gains in DoA estimation and is able to resolve angles with RMSE $\simeq 0.5^{\circ}$ in cases where the conventional approach fails ($T = 16$).
- One of the main advantages is that for the DoA estimation the method is not limited to the use of MUSIC. Any other estimator can be used, e.g., Root-MUSIC, a classification neural network, etc.

Conclusions

- We presented a novel deep learning approach for DoA estimation for 1) low SNR, 2) small number of snapshots T, and we focused on the overdetermined ($K < N - 1$) and underdetermined case ($K \geq N$) using the ULA and MISC arrays, respectively.
- The problem is formulated as a manifold learning task and a (deep) denoising autoencoder architecture is trained for the prediction of the true (unknown) manifold. The DoA estimation follows with the use of a conventional covariance-based technique.
- The adopted approach demonstrates significant performance gains in DoA estimation and is able to resolve angles with RMSE $\simeq 0.5^{\circ}$ in cases where the conventional approach fails ($T = 16$).
- One of the main advantages is that for the DoA estimation the method is not limited to the use of MUSIC. Any other estimator can be used, e.g., Root-MUSIC, a classification neural network, etc.

Conclusions

- We presented a novel deep learning approach for DoA estimation for 1) low SNR, 2) small number of snapshots T, and we focused on the overdetermined ($K < N - 1$) and underdetermined case ($K \geq N$) using the ULA and MISC arrays, respectively.
- The problem is formulated as a manifold learning task and a (deep) denoising autoencoder architecture is trained for the prediction of the true (unknown) manifold. The DoA estimation follows with the use of a conventional covariance-based technique.
- The adopted approach demonstrates significant performance gains in DoA estimation and is able to resolve angles with RMSE $\simeq 0.5^{\circ}$ in cases where the conventional approach fails ($T = 16$).
- One of the main advantages is that for the DoA estimation the method is not limited to the use of MUSIC. Any other estimator can be used, e.g., Root-MUSIC, a classification neural network, etc.

Conclusions

- We presented a novel deep learning approach for DoA estimation for 1) low SNR, 2) small number of snapshots T, and we focused on the overdetermined ($K < N - 1$) and underdetermined case ($K \geq N$) using the ULA and MISC arrays, respectively.
- The problem is formulated as a manifold learning task and a (deep) denoising autoencoder architecture is trained for the prediction of the true (unknown) manifold. The DoA estimation follows with the use of a conventional covariance-based technique.
- The adopted approach demonstrates significant performance gains in DoA estimation and is able to resolve angles with RMSE $\simeq 0.5^{\circ}$ in cases where the conventional approach fails ($T = 16$).
- One of the main advantages is that for the DoA estimation the method is not limited to the use of MUSIC. Any other estimator can be used, e.g., Root-MUSIC, a classification neural network, etc.

References

1. George Papageorgiou, M. Sellathurai, "Fast Directions-of-arrival estimation of multiple targets using deep learning and sparse arrays", ICASSP May 2020.
2. Papageorgiou, M. Sellathurai, "Direction-of-Arrival Estimation in the Low-SNR Regime via a Denoising Autoencoder", SPAWC June 2020.
3. George Papageorgiou, M. Sellathurai, Y. Eldar Deep Networks for Direction-of-Arrival Estimation in Low SNR, submitted to Transactions on SIgnal Processing, https://arxiv.org/abs/2011.08848
4. P. Pal and P. P. Vaidyanathan, "Coprime sampling and the MUSIC algorithm," *in Proc. Digital Signal Process. Signal Process. Educ. Meeting*, Sedona, AZ, USA, pp. 289–294, Jan. 2011.
5. Z. Zheng, W. Q. Wang, Y. Kong, and Y. D. Zhang, "MISC Array: A New Sparse Array Design Achieving Increased Degrees of Freedom and Reduced Mutual Coupling Effect," *IEEE Trans. Signal Process.*, vol. 67, no. 7, pp. 1728–1741, 2019.

THANK YOU AND QUESTIONS TIME

For further questions or any other inquiries please send us an email:
m.sellathurai@hw.ac.uk